LEGIBILITY NOTICE

A major purpose of the Technical Information Center is to provide the broadest dissemination possible of information contained in DOE's Research and Development Reports to business, industry, the academic community, and federal, state and local governments.

Although a small portion of this report is not reproducible, it is being made available to expedite the availability of information on the research discussed herein.

LA-UR -90-537

Los Alamos National Laboratory is operated by the University of California for the United States Department of Energy under contract W-7405-ENG-36

LA-UR--90-537

DE90 007540

TITLE: **INTEGRABILITY AND CHAOS IN NONLINEARLY COUPLED OPTICAL BEAMS**

AUTHOR(S): **D. DAVID**

SUBMITTED TO: **The Proceedings of the C.R.M. Workshop on Hamiltonian Systems, Transformation Groups and Spectral Transform Methods, held at the University of Montreal, Montreal Canada, October 20-26, 1989**

DISCLAIMER

Los Alamos National Laboratory
Los Alamos, New Mexico 87545

INTEGRABILITY AND CHAOS IN NONLINEARLY COUPLED OPTICAL BEAMS

D. David
Center for Nonlinear Studies & T Division, MS B258
Los Alamos National Laboratory
Los Alamos, NM 87545

Abstract. This paper presents a study, using dynamical systems methods, of the equations describing the polarization behaviour of two nonlinearly coupled optical beams counterpropagating in a nonlinear medium. In the travelling-wave regime assumption, this system possesses a Lie-Poisson structure on the manifold $C^2 \times C^2$. In the case where the medium is assumed to be isotropic, this system exhibits invariance under the Hamiltonian action of two copies of the rotation group, S^1, and actually reduces to a lower–dimensional system on the two-sphere, S^2. We study the dynamics on the reduced space and examine the structure of the phase portrait by determining the fixed points and infinite–period homoclinic and heteroclinic orbits; we concentrate on presenting some exotic behaviour that occurs when some parameters are varied, and we also show special solutions associated with some of the above–mentioned orbits. Last, we demonstrate the existence of complex dynamics when the system is subject to certain classes of Hamiltonian perturbations. To this end, we make use of the Melnikov method to analytically show the occurence of either horseshoe chaos, or Arnold diffusion.

1. Introduction. Integrable Hamiltonian systems often exhibit a transition to chaotic, or complex, behaviour when they are subject to small periodic perturbations. In low-dimensional cases (e.g., a one-degree-of freedom system), chaoticity usually shows its presence in the form of Smale horseshoes in the structure of the associated Poincaré map. This structure is inherently characterized by combined stretching and folding in the above map, as well as an invariant Cantor-like set as the infinite–time iterate of this map. A method, first developed by Melnikov [1963] and Arnold [1964], and later developed further for extended types of systems by Holmes and Marsden [1982a] and Wiggins [1988], is the tool that is used here to establish in an analytical way that, for the perturbed systems considered in this paper, iterating the Poincaré map indeed implies the existence of a horseshoe structure, by virtue of the Melnikov and Poincaré–Birkhoff–Smale theorems. If the dimensionality of the system is high enough, an additional feature may take place, Arnold diffusion, as a signature that the KAM torii are insufficient to confine orbits within a single region of chaoticity. This can occur through resonance overlaps, thus giving rise to Arnold webs (or transition chains).

The dynamics that we will discuss here concerns the Hamiltonian description of the travelling–wave dynamics of polarized, nearly monochromatic, optical laser pulses counter-propagating in a lossless, cubically nonlinear, parity–invariant, anisotropic, homogeneous medium; for instance, polarized beams in a straight optical fiber constitutes a realization of such a system. Our approach will use the method of dimensional reduction for Hamiltonian systems with a continuous Lie point-group of symmetries, together with the Melnikov–Arnold method to show the existence of complex behaviour under certain small perturbations, induced by modulating the optical parameters characterizing the medium of propagation.

Nonlinear polarization dynamics of optical laser pulses is a subject which has been under investigation for a few decades. Some 25 years ago, Maker *et al.* [1964] analyzed and demonstrated the precession of the polarization ellipse for a single beam propagating in a nonlinear medium. Spatially stable solution configurations for the problem of the interaction of two counterpropagating beams in an isotropic medium were considered in Kaplan [1983] and Lytel [1984]. The phenomenon of optical multi–stability is is also studied in Lytel [1984], and in Otsuka*et al.* [1985]. Reports of numerical evidence for chaotic behaviour and interpretations of experimental data can be found in Trillo *et al.* [1986] and Gaeta *et al.* [1987]. Previous work on special solutions for the one–beam and the two–beam problems appear in Tratnik and Sipe [1987]. Additional references and more detailed treatment of Hamiltonian chaos in nonlinear optical polarization dynamics can be found in David [1989] and in David *et al.* [1988a, 1988b, 1990].

The plan of this paper is as follows. In Section 2 we formulate the polarization dynamics of travelling–wave optical pulses in Hamiltonian form; this is done in terms of two complex 2–component envelope electric field variables. In Section 3, after a convenient change of variables, we use the method of reduction for Hamiltonian systems with symmetry to effectively recast the problem as a more tractable system on a lower–dimensional phase space, namely the sphere. This is actually achieved in two steps, each involving a rotational invariance. The first step transports the system from the initial phase space $C^2 \times C^2$ to $S^2 \times S^2$; the second step takes advantage of the isotropy property of the propagation medium and finally brings the problem down to S^2. Specifically, these reduction steps are taken by restricting to level sets of first integrals of the systems, and then by projecting to the space obtained by quotienting by the residual Hamiltonian invariance

group. Section 4 is devoted to the qualitative analysis of the reduced system for a few special cases. Specifically, we classify the fixed points of the reduced dynamics on the sphere and describe the various bifurcations involving these points that take place as material parameters and intensities of the beams are varied. Some degeneracies occur during the second reduction step and lead to peculiar bifurcations; we describe these in detail. Special soliton-like and kink-like solutions are also depicted. In Section 5, we use the Melnikov method to demonstrate how homoclinic (or heteroclinic) orbits tangle and break up to yield complex behaviour when the dynamics is perturbed by modulated material inhomogeneities, modelled as spatially periodic variations of the optical parameters of the medium. Conclusions of this study are summarized in the final Section 6.

2. Physical formulation of the problem. The travelling-wave evolution of the polarization dynamics of our system of two counterpropagating beams involves complex electric field amplitudes $e_i(\tau)$ and $\bar{e}_i(\tau)$, appearing in the following eikonal form,

$$E_i(z,\tau) = \left[e_i(z,\tau)e^{ikz} + \bar{e}_i(z,\tau)e^{-ikz}\right] e^{-i\omega t} + c.c. \tag{2.1}$$

where $\tau = z - ct$ is the travelling-wave variable and where $i = 1,2$ is the polarization index. We note that each of $\mathbf{e}$ and $\bar{\mathbf{e}}$ are elements of C^2. Also, here and below, the "bars" are used to distinguish between quantities associated with one beam or the other. The third-order nonlinear polarizability is written as

$$P_i(z,t) = \chi^{(1)}_{ij} * E_j + \chi^{(3)}_{ijk\ell} * E_j E_k E_\ell \tag{2.2}$$

where $*$ indicates convolution with respect to time and we sum over repeated indices. Using the rotating wave approximation in Maxwell's equations and assuming a lossless medium, small nonlinear anisotropy $\chi^{(3)}$ and null $\chi^{(1)}$ (corresponding to considering an anisotropic and parity-invariant medium), slowly varying amplitudes, and a far-away-from-resonance situation, we obtain the following set of equations governing the dynamics of the electric field amplitudes:

$$\begin{aligned} i\dot{e}_j &= \frac{i\bar{\kappa}}{\bar{r}}\chi^{(3)}_{jk\ell m} e_k (e_\ell e^*_m + 2\bar{e}_k \bar{e}^*_\ell), \\ i\dot{\bar{e}}_j &= \frac{i\kappa}{r}\chi^{(3)}_{jk\ell m} \bar{e}_k (\bar{e}_\ell \bar{e}^*_m + 2e_k e^*_\ell). \end{aligned} \tag{2.3}$$

where the constant susceptibility tensor $\chi^{(3)}$ satisfies the following involutions:

$$\chi^{(3)}_{ijk\ell} = \chi^{(3)*}_{ji\ell k}, \qquad \chi^{(3)}_{ijk\ell} = \chi^{(3)}_{\ell jki} = \chi^{(3)}_{ikj\ell}. \tag{2.4}$$

These equations constitute a quasi–canonical Hamiltonian system on $C^2 \times C^2$. The Hamiltonian function is

$$H(\mathbf{e}, \bar{\mathbf{e}}) = \tfrac{1}{8}\chi^{(3)}_{ijk\ell}\left[e^*_i e_j e_k e^*_\ell + 4e^*_i e_j \bar{e}_k \bar{e}^*_\ell + \bar{e}^*_i \bar{e}_j \bar{e}_k \bar{e}^*_\ell\right], \tag{2.5}$$

with the associated Hamiltonian vector field

$$X_H = \frac{i\bar{\kappa}}{\bar{r}}(\nabla_{e^*} H \cdot \nabla_e - \nabla_e H \cdot \nabla_{e^*}) + \frac{i\kappa}{r}(\nabla_{\bar{e}^*} H \cdot \nabla_{\bar{e}} - \nabla_{\bar{e}} H \cdot \nabla_{\bar{e}^*}). \tag{2.6}$$

so that any dynamical quantity Q evolves according to the prescription

$$\dot{Q} = X_H Q \qquad (= \{Q, H\}). \tag{2.7}$$

This endows the phase space, $(C^2 \times C^2, \{\cdot,\cdot\})$, with a Lie–Poisson structure.

3. Reduction to S^2. Generically, Hamiltonian systems defined on high–dimensional manifolds are somewhat difficult to study because, for one thing, it proves virtually impossible to characterize the geometry of the phase space in any way that is easy to grasp. It is often very convenient to use any continuous symmetry the system may possess in order to redefine it onto a new space with less dimensions. Such a technique is used, for instance, to help one to find solutions of difficult nonlinear partial differential equations by reducing them to equations with fewer variables; these yield so–called (sub) group–invariant solutions. Along the same lines, a Hamiltonian dynamical system can also be reduced, to a system on a lower–dimensional phase space (i.e., to a set of equations with fewer dependent variables) if it is possesses symmetries. This allows for a study of the dynamics on the reduced phase space, after which one may revert to the original space to deduce results pertinent to the variables in terms of which the problem was defined. The machinery lying behind the method of Hamiltonian symmetry reduction is based upon the following theorem (see ,e.g., Chapter 6 of Olver [1986] for details). Let $\mathcal{G}$ be a Hamiltonian symmetry group of transformations acting on $\mathcal{M}$ and generated by a set $\{P_i\}$ of first integrals. We define the momentum map $\mathcal{P} : \mathcal{M} \longrightarrow g^* : x \longmapsto \sum P_i(x)\omega_i$, where $\{\omega_i\}$ is a basis of g^*,

the dual to the Lie algebra of the group $\mathcal{G}$. We denote by S_α the common α-level set of $\mathcal{P}$. The residual symmetry group $\mathcal{G}_\alpha$ on S_α is the isotropy subgroup of $\alpha \in g^*$.

Reduction Theorem. *Let $\mathcal{P}$ be of maximal rank everywhere on S_α and let $\mathcal{G}_\alpha$ act regularly on the submanifold S_α. Then there is a natural induced immersion $\phi : S_\alpha/\mathcal{G}_\alpha \hookrightarrow \mathcal{M}/\mathcal{G}$ such that $S_\alpha/\mathcal{G}_\alpha$ is a Poisson submanifold so that the diagram*

$$\begin{array}{ccc} & \overset{i}{\hookrightarrow} & \\ S_\alpha & & \mathcal{M} \\ \Big\downarrow{\scriptstyle \pi_\alpha} & & \Big\downarrow{\scriptstyle \pi} \\ S_\alpha/\mathcal{G}_\alpha & \underset{\phi}{\hookrightarrow} & \mathcal{M}/\mathcal{G} \end{array}$$

commutes. π and π_α are the natural projections and i i.e. immersion realizing S_α as a submanifold of $\mathcal{M}$. Moreover, any Hamiltonian system on $\mathcal{M}$ with $\mathcal{G}$ as a symmetry group naturally restricts to Hamiltonian systems on $S_\alpha/\mathcal{G}_\alpha$ and $\mathcal{M}/\mathcal{G}$.

In practice, in order to prevent reconstructibility problems, the above theorem suggests that one may reduce to the space $S_\alpha/\mathcal{G}_\alpha$ by first restricting to S_α and then projecting via π_α. For the system (2.3) under consideration here, two S^1 invariances will allow us to perform reduction. First, it proves convenient to make a change of variables on $C^2 \times C^2$ by reparametrizing this space with Stokes variables, as follows:

$$\begin{aligned} \mathbf{u} &= \mathbf{e}^\dagger \vec{\sigma} \mathbf{e}, \qquad u_0 \equiv r = \mathbf{e}^\dagger \cdot \mathbf{e}, \\ \overline{\mathbf{u}} &= \overline{\mathbf{e}}^\dagger \vec{\sigma} \overline{\mathbf{e}}, \qquad \overline{u}_0 \equiv \overline{r} = \overline{\mathbf{e}}^\dagger \cdot \overline{\mathbf{e}}. \end{aligned} \tag{3.1}$$

where $\vec{\sigma} = (\sigma_3, \sigma_1, \sigma_2)$ are the usual Pauli matrices. One observes that both u_0 and $\overline{u}_0$ are first integrals of the motion and are associated with the invariance of the system under the rotation transformation $(\mathbf{e}, \overline{\mathbf{e}}) \mapsto e^{i\theta}(\mathbf{e}, \overline{\mathbf{e}})$. Our first step, in accord with the above theorem, is to restrict to an immersed common level set $u_0 = r, \overline{u}_0 = \overline{r}$. Let us write $\mathbf{e}$ and $\overline{\mathbf{e}}$ as

$$\mathbf{e} = (e_1, e_2) = (x_1 + ix_2, x_3 + ix_4), \quad \overline{\mathbf{e}} = (\overline{e}_1, \overline{e}_2) = (\overline{x}_1 + i\overline{x}_2, \overline{x}_3 + i\overline{x}_4) \tag{3.2}$$

It is then easy to see that $u_0 = x_1^2 + x_2^2 + x_3^2 + x_4^2$ and $\overline{u}_0 = \overline{x}_1^2 + \overline{x}_2^2 + \overline{x}_3^2 + \overline{x}_4^2$; thus the level set is simply $S^3 \times S^3$. On this space, the Hamiltonian function, the Hamiltonian vector

field, and the equations of motion become

$$H(\mathbf{u},\overline{\mathbf{u}}) = \tfrac{1}{2}(\mathbf{u}\cdot\mathbf{W}\cdot\mathbf{u} + \overline{\mathbf{u}}\cdot\mathbf{W}\cdot\overline{\mathbf{u}}) + 2\overline{\mathbf{u}}\cdot\mathbf{W}\cdot\mathbf{u}, \tag{3.3a}$$

$$X_H = \frac{\overline{\kappa}}{\overline{r}}(\nabla_{\mathbf{u}}H\times\mathbf{u})\cdot\nabla_{\mathbf{u}} + \frac{\kappa}{r}(\nabla_{\overline{\mathbf{r}}}H\times\overline{\mathbf{u}})\cdot\nabla_{\overline{\mathbf{u}}}, \tag{3.3b}$$

$$\dot{\mathbf{u}} = \frac{\overline{\kappa}}{\overline{r}}[\mathbf{W}\cdot(\mathbf{u}+2\overline{\mathbf{u}})]\times\mathbf{u}, \quad \dot{\overline{\mathbf{u}}} = \frac{\kappa}{r}[\mathbf{W}\cdot(\overline{\mathbf{u}}+2\mathbf{u})]\times\overline{\mathbf{u}}, \tag{3.3c}$$

where

$$\mathbf{W} = \vec{\sigma}_{ij}\chi^{(3)}_{ijk\ell}\vec{\sigma}_{k\ell} = \mathrm{Diag}(\lambda_1,\lambda_2,\lambda_1)\,. \tag{3.4}$$

One can always perform a transformation such that the matrix $\mathbf{W}$ will be diagonal. The components of $\mathbf{W}$ are interaction terms of the following types: W_{11}, W_{13}, W_{33} are linear–linear polarization interaction terms, W_{12}, W_{23} are linear–circular polarization interaction terms, and W_{22} is a circular–circular polarization interaction term. Note that the isotropy condition mentioned earlier makes the first and third components equal. Now, using the representation (3.2), we notice that the components of $\mathbf{u}$ and $\overline{\mathbf{u}}$ write as

$$\begin{aligned}
u_3 &= 2(x_1x_3 + x_2x_4), & \overline{u}_3 &= 2(\overline{x}_1\overline{x}_3 + \overline{x}_2\overline{x}_4),\\
u_1 &= 2(x_1x_4 - x_2x_3), & \overline{u}_1 &= 2(\overline{x}_1\overline{x}_4 - \overline{x}_2\overline{x}_3),\\
u_2 &= x_1^2 + x_2^2 - x_3^2 - x_4^2, & \overline{u}_2 &= \overline{x}_1^2 + \overline{x}_2^2 - \overline{x}_3^2 - \overline{x}_4^2.
\end{aligned} \tag{3.5}$$

The above formulae (3.5) constitute the transformation $S^3 \mapsto S^2$ due to Hopf (see, e.g., Crampin and Pirani [1987]). We then notice that the components of $\mathbf{u}$ and $\overline{\mathbf{u}}$ are not all independent; indeed, we have

$$u_1^2 + u_2^2 + u_3^2 = r^2, \qquad \overline{u}_1^2 + \overline{u}_2^2 + \overline{u}_3^2 = \overline{r}^2. \tag{3.6}$$

Thus, we realize that we are dealing with the manifold $S^2 \times S^2$, since each equation in (3.6) actually defines a sphere. Each copy of S^2 in the above product is sometimes referred to as a *Poincaré sphere* (see Figure 1). Points on this sphere represent polarization states: the poles are circularly polarized states, equatorial points correspond to linearly polarized states, and all other points describe elliptical states. We are choosing the north and south poles to lie along the 2-axis to conform with optics notation.

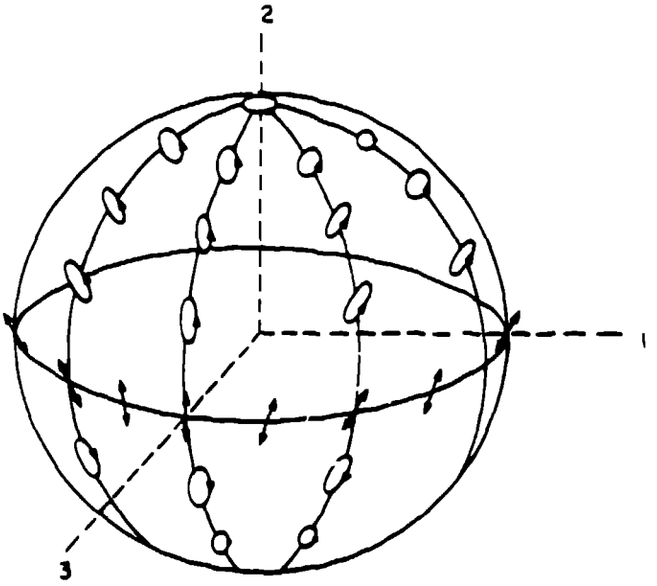

Figure 1. The Poincaré sphere.

To actually reduce on $S^2 \times S^2$, we use spherical coordinates,

$$\begin{aligned} u_1 &= r\sin\theta\sin\phi, & \bar{u}_1 &= \bar{r}\sin\bar{\theta}\sin\bar{\phi}, \\ u_2 &= r\cos\theta, & \bar{u}_2 &= \bar{r}\cos\bar{\theta}, \\ u_3 &= r\sin\theta\cos\phi, & \bar{u}_3 &= \bar{r}\sin\bar{\theta}\cos\bar{\phi}, \end{aligned} \tag{3.7}$$

In terms of these coordinates, the Hamiltonian function, X_H, and the equations of motion take the following form:

$$\begin{aligned} H(\theta,\phi,\bar{\theta},\bar{\phi}) = {}& \tfrac{1}{2}r^2\left[\lambda_1\sin^2\theta + \lambda_2\cos^2\theta\right] + \tfrac{1}{2}\bar{r}^2\left[\lambda_1\sin^2\bar{\theta} + \lambda_2\cos^2\bar{\theta}\right] \\ & + 2r\bar{r}\left[\lambda_1\sin\theta\sin\bar{\theta}\cos(\phi-\bar{\phi}) + \lambda_2\cos\theta\cos\bar{\theta}\right], \end{aligned} \tag{3.8a}$$

$$X_H = \frac{\bar{\kappa}}{r\bar{r}\sin\theta}\left[H_\phi\partial_\theta - H_\theta\partial_\phi\right] + \frac{\kappa}{r\bar{r}\sin\bar{\theta}}\left[H_{\bar{\phi}}\partial_{\bar{\theta}} - H_{\bar{\theta}}\partial_{\bar{\phi}}\right], \tag{3.8b}$$

$$\dot{\theta} = -2\lambda_1\bar{\kappa}\sin\bar{\theta}\sin(\phi-\bar{\phi}), \tag{3.8c}$$

$$\dot{\bar{\theta}} = 2\lambda_1\kappa\sin\theta\sin(\phi-\bar{\phi}), \tag{3.8d}$$

$$\dot{\phi} = \frac{\bar{\kappa}\bar{r}}{r}(\lambda_2-\lambda_1)\cos\theta - 2\bar{\kappa}\left(\lambda_1\cos\theta\frac{\sin\bar{\theta}}{\sin\theta}\cos(\phi-\bar{\phi}) - \lambda_2\cos\bar{\theta}\right), \tag{3.8e}$$

$$\dot{\bar{\phi}} = \frac{\kappa\bar{r}}{r}(\lambda_2-\lambda_1)\cos\bar{\theta} - 2\kappa\left(\lambda_1\cos\bar{\theta}\frac{\sin\theta}{\sin\bar{\theta}}\cos(\phi-\bar{\phi}) - \lambda_2\cos\theta\right). \tag{3.8f}$$

We now proceed with the second step of the reduction. Notice that the quantity $\sigma = \kappa\cos\theta + \overline{\kappa}\cos\overline{\theta}$ is also a constant of the motion. A level set is thus a three–dimensional manifold specified by a constant value of σ and is coordinatized, for instance, by triplets $(\phi, \overline{\phi}, \omega)$ where $\omega = \kappa\cos\theta - \overline{\kappa}\cos\overline{\theta}$. At this point, we make the following remark. Recall that the reduction theorem necessitates that the momentum be of maximal rank. Here, this means that we will have degenerate situations when the function $\sigma(\theta, \overline{\theta})$ will not be of maximal rank, i.e., when $\sin\theta = \sin\overline{\theta} = 0$. This corresponds to $\sigma = \pm(|\kappa| + |\overline{\kappa}|)$ and $\sigma = \pm(|\kappa| - |\overline{\kappa}|)$. The first two cases are venial; they correspond to the extreme values possible for σ and the dynamics then reduces to a point (physically, this is achieved when the polarizations of the beams are aligned alond the polar direction: this configuration is forever the same). As for the two other situations, they physically arise when the polarizations of the beams are anti–aligned along the polar direction and will yield degeneracies in the phase portraits, as we will observe later in Section 4. Now, we also note that the residual symmetry group S_σ is again S^1 and its Lie algebra is generated by the vector field

$$X_\sigma = \frac{\kappa\overline{\kappa}}{r\overline{r}}\left(\partial_\phi - \partial_{\overline{\phi}}\right). \tag{3.9}$$

This suggests that we pick the following new coordinates:

$$\alpha = \phi - \overline{\phi}, \quad \beta = \phi + \overline{\phi}, \quad \omega = \omega_0 + R\cos\psi \tag{3.10}$$

where ψ is defined through three different formulae according to the relative magnitude of the constant σ:

$$1)\ \sigma \geq\ |\overline{\kappa}| - |\kappa|: \qquad \cos\psi\ =\ \frac{|\overline{\kappa}|\left(1-\cos\overline{\theta}\right) - |\kappa|\left(1-\cos\theta\right)}{|\overline{\kappa}|\left(1-\cos\overline{\theta}\right) + |\kappa|\left(1-\cos\theta\right)} \tag{3.11a}$$

$$2)\ |\kappa| - |\overline{\kappa}|\ \leq \sigma \leq\ |\overline{\kappa}| - |\kappa|: \qquad \cos\psi\ =\ \cos\theta, \tag{3.11b}$$

$$3)\ \sigma \leq\ |\kappa| - |\overline{\kappa}|: \qquad \cos\psi\ =\ \frac{|\kappa|\left(1+\cos\theta\right) - |\overline{\kappa}|\left(1+\cos\overline{\theta}\right)}{|\kappa|\left(1+\cos\theta\right) + |\overline{\kappa}|\left(1+\cos\overline{\theta}\right).} \tag{3.11c}$$

The constants ω_0 and R are determined by using (3.10). Writing down the expressions for the Hamiltonian function of the system and the Hamiltonian vector field gives

$$H(\alpha, \omega(\phi)) = \tfrac{1}{2}\lambda_1\{r^2 + \overline{r}^2 + \frac{r\overline{r}}{\kappa\overline{\kappa}}\left[\Gamma\omega^2 + \Delta\sigma^2 + E\sigma\omega + f(\psi)\overline{f}(\psi)\cos\alpha\right]\}, \tag{3.12a}$$

$$X_H = \frac{2\kappa\overline{\kappa}}{r\overline{r}R\sin\psi}\left[H_\alpha\partial_\psi - H_\psi\partial_\alpha\right] + \frac{2\kappa\overline{\kappa}}{r\overline{r}}H_\sigma\partial_\beta, \tag{3.12b}$$

where

$$\Gamma = \tfrac{1}{4}(L-1)\rho_+ - L, \quad \Delta = \tfrac{1}{4}(L-1)\rho_+ + L, \quad E = \tfrac{1}{4}(L-1)\rho_-, \tag{3.12c}$$

$$L = \lambda_2/\lambda_1, \qquad \rho_\pm = (r\overline{\kappa}/\overline{r}\kappa \pm \overline{r}\kappa/r\overline{\kappa}), \tag{3.12d}$$

$$f(\psi) = \sqrt{4\kappa^2 - (\sigma+\omega)^2}, \quad \overline{f}(\psi) = \sqrt{4\overline{\kappa}^2 - (\sigma-\omega)^2}. \tag{3.12e}$$

As for the equations of motion, we find them to be

$$\dot{\psi} = \frac{\lambda_1 \sin\alpha}{R\sin\psi} f(\psi)\overline{f}(\psi), \tag{3.13a}$$

$$\dot{\alpha} = \lambda_1(2\Gamma\omega + E\sigma) + \lambda_1[(\sigma-\omega)f(\psi)/\overline{f}(\psi) - (\sigma+\omega)\overline{f}(\psi)/f(\psi)]\cos\alpha, \tag{3.13b}$$

$$\dot{\beta} = \lambda_1(2\Delta\sigma + E\omega) - \lambda_1[(\sigma-\omega)f(\psi)/\overline{f}(\psi) + (\sigma+\omega)\overline{f}(\psi)/f(\psi)]\cos\alpha, \tag{3.13c}$$

A few remarks are in order. First, we observe that the variable β does not appear in the equations for the variables α and ψ, thus confirming that we reduced to S^2; indeed we can solve for the two latter quantities and then get the former through a quadrature of (3.13c). A second remark concerns the degeneracies mentioned earlier. When $\sigma = \pm(\kappa - \overline{\kappa})$, either one of the poles on the sphere will be singular, or both of them if, in addition, $\sigma = 0$. This indicates that the phase space could actually be viewed as a pierced sphere with one or both removed. A last comment is to the effect that the unreduced system is completely integrable; this is a consequence of the fact that the reduced phased space is two-dimensional, i.e., that the reduced system possesses a single degree of freedom. Moreover, the solution manifold of the unreduced system (2.3) is completely determined from that of the reduced system (3.13a,b) on S^2.

4. Phase portrait analysis. In this section, we will investigate the nature of the phase portrait for the reduced system (3.13a,b). Specifically, we will limit ourselves to a few particularly interesting subcases (more details about the existence and the description of bifurcation sequences for both the one–beam and the two–beam problems can be found in David *et al.*[1990]) and wish to determine the fixed points and determine their type; since we are dealing with a Hamiltonian system, the fixed points can only be stable *centers* or unstable *saddle points*, although some exotic points may arise as *pseudo critical points* when degenerate bifurcations take place. An additional feature of the phase space is the possible existence, aside from periodic trajectories, of infinite–period orbits. These, on one

hand, provide us with especially interesting solutions, and on the other hand, are a prime ingredient when looking for chaotic behaviour.

Case 1 $\bar{r} = r, |\bar{\kappa}| = |\kappa|$. We also mention that setting $\sigma = 0$ and $|\bar{\kappa}| \neq |\kappa|$ also yields the same dynamics. The geometry of the phase portrait depends on two essential parameters, Γ and σ and is depicted in Figure 2. For sufficiently large magnitudes of $|\Gamma|$, and for $\sigma \neq 0$, the sphere is partitioned into three distinct families of periodic orbits, with three limit stable fixed points, separated by a pair of homoclinic loops connected to a hyperbolic saddle point; we thus have a figure–eight pattern. Asymptotically, as $|\Gamma| \to \infty$, the above loops merge to a great circle of fixed points on the equator. As $|\Gamma|$ gets smaller, these homoclinic loops shrink and eventually collapse to the saddle point as $|\Gamma| \to \Gamma_{\pm}(\sigma)$, at which point a reverse bifurcation takes place, i.e., (Saddle + 2 Centers) $\to$ (Center). The curves on the (Γ, σ)–plane on which the bifurcation occurs are parabolas given by

$$\Gamma_{\pm}(\sigma) = \frac{\sigma^2 + 4\kappa^2}{\sigma^2 - 4\kappa^2} \tag{4.1}$$

The limit $\sigma \to 0$ is special and corresponds to a degeneracy mentioned earlier, where the reduced phase space actually consists of S^2 without its two poles. When $\sigma = 0$, we observe that the poles behave as fixed points, irrespective of the value of Γ. Examining Figure 2, we then see that the homoclinic loops in the phase portrait cannot shrink to the saddle point because the two centers they enclose are constrained to remain at the poles. So these loops actually collapse to form a half great–circle of fixed points from one pole to the other. As the critical parabolic curve is traversed, the nature of the bifurcation is naturally also degenerate: the two *pseudo fixed points* at the poles see their type change to saddles, whereas the saddle point on the equator becomes a stable point. In addition, the line of fixed points opens up into two geodesics between the poles that act as heteroclinic trajectories (infinite period).

In Figure 3, we illustrate some special solutions associated with trajectories of infinite period appearing in Figure 2. These curves are drawn on the u–Poincaré sphere and show how the polarization evolves with time. The left picture corresponds to any of the two geodesic heteroclinic lines connecting the poles: the polarization ellipse describing the beam starts as a circle and then sees its eccentricity increase as it rotates about its center, until it ends up as a line when the trajectory gets to the equator on the Poincaré sphere. The two other pictures correspond to the homoclinic loops appearing in Figure 2 for the

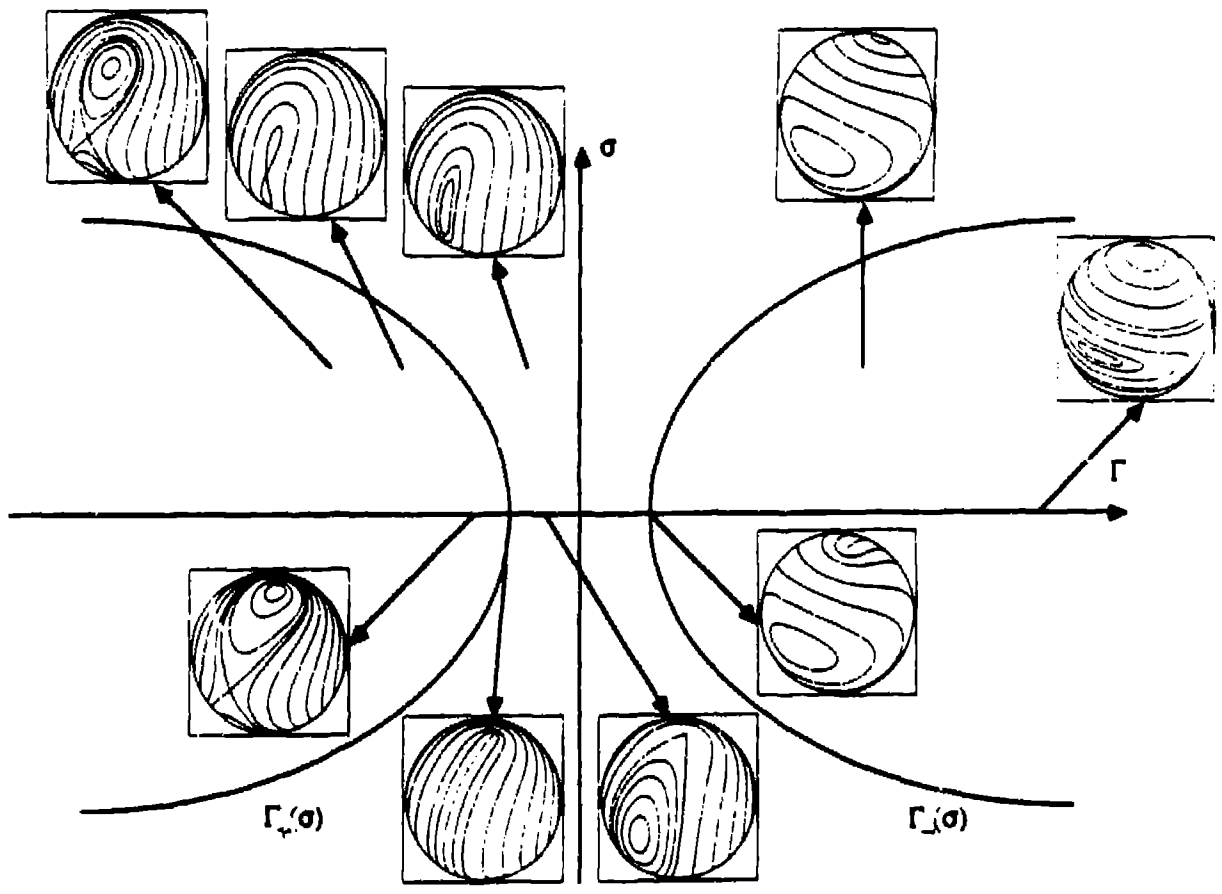

Figure 2. The phase portrait for case 1. A degenerate bifurcation takes place when $\sigma = 0$.

non–degenerate situation. Typically, on the Poincaré sphere, these orbits correspond to trajectories that originate on the equator (thus an initial linearly polarization state) and spiral around one of the poles for any number of times before going back to the equator. These solutions are reminiscent of kinks; in the particular case when they get back to their initial location, they are identified as solitary waves.

Case 2 $\overline{\tau} = \pm(|\overline{\kappa}| - |\kappa|)$. This second case also exhibits interesting features. The singular situation ($\sigma = 0$) from the previous case is also obtained as a limit when $|\overline{\kappa}| = |\kappa|$. Again, the equations of motion imply a special fixed point, constrained to be located at one pole, irrespective of the parameters. We illustrate the bifurcation behaviour in Figure 4. When the magnitude of $|\Gamma|$ is sufficiently large the phase portrait consists of a family of

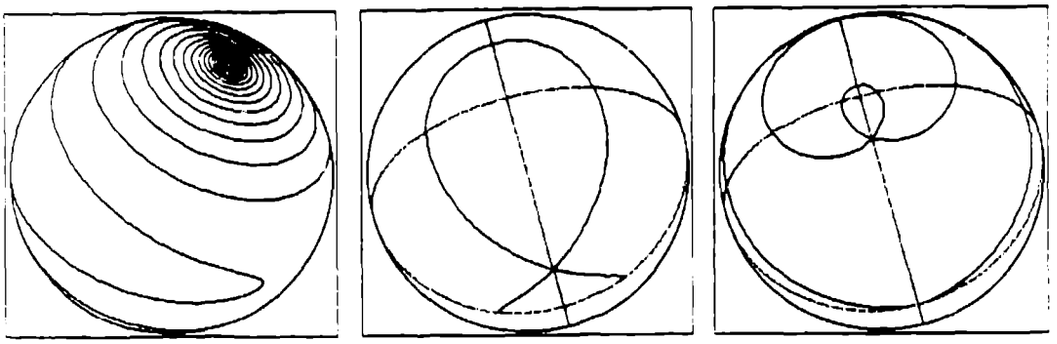

Figure 3. Some special kink-like and soliton-like solutions associated with infinite-period orbits appearing in Figure 2.

periodic orbits with two stable fixed points, one exactly at the north pole and the other one nearby the south pole. Nothing happens qualitatively to this description until $|\Gamma|$ reaches a critical value, at which point the north pole becomes unstable and this is accompanied by the creation of a single loop homoclinic to the pole As Γ crosses zero and changes sign, this loop stretches, goes under the sphere, and eventually shrinks to the north pole, but from the opposite direction to which it emerged from. We also note that during the evolution of this loop, the stable center it initially enclosed was left to stay nearby the south pole, while it dragged the center initially located near the south pole to collapse with it at the north pole.

Let us make the following closing remark for this Section. The Euler index on a surface is definedas the difference between the number of stable and unstable fixed points present in the phase portrait; this number is an invariant. For the two-sphere, S^2, this number is equal to two (it is unity for the real plane). We observe that the index is indeed 2 for all the phase space configurations except when a singular situation occurs, which is just another indication that tells us that the reduced phase space is singular. For the degenerate subcase of case 1, the index is zero (two extra pseudo saddle points at the poles) and it is one for case 2 (one extra hyperbolic point at the north pole).

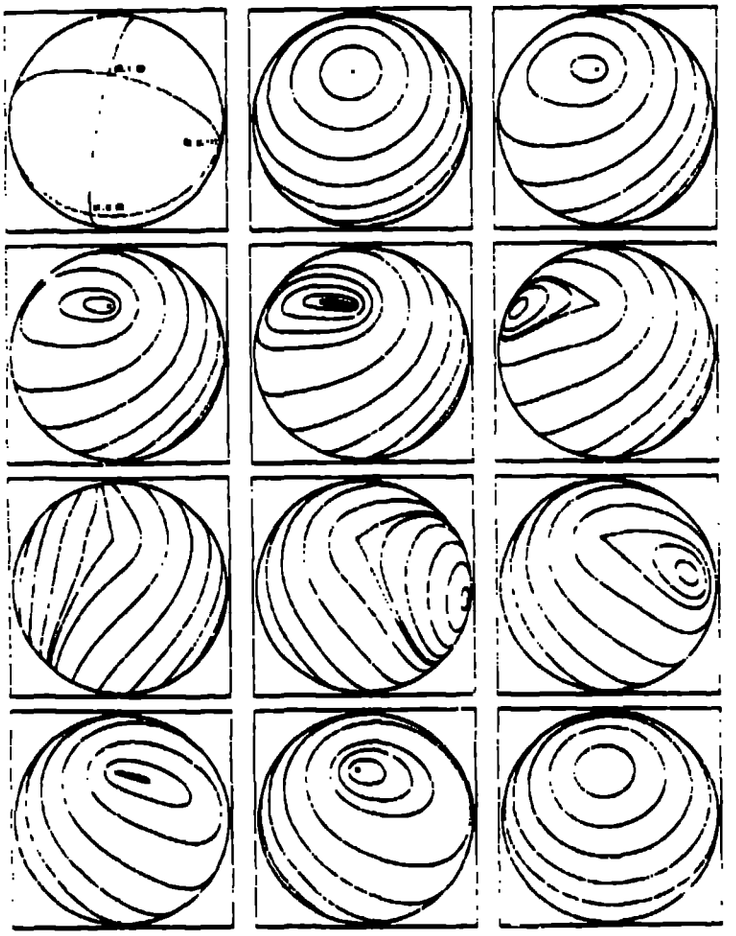

Figure 4. Bifurcation behaviour for case 2. Note the presence of a single homoclinic loop connected with one of the poles.

5. Homoclinic chaos. In this section, we will investigate the question of generating complex dynamics for our system when it is subject to some classes of perturbations. These consist in modifying the material parameters of the optical medium in certain specific ways. These perturbations are of physical relevance in applied fields such as fiber optics communications and polarization switching. We will use the Melnikov technique (see Melnikov [1963], Guckenheimer and Holmes [1983], and Wiggins [1988]) to demonstrate the existence of chaos for our optical system, in the form of either horseshoe structures or Arnold diffusion when the dimension is high enough. This method essentially relies on showing that the stable and unstable manifolds of certain hyperbolic manifolds do intersect

transversely. This is actually done by calculating so–called Melnikov integral functions, which approximate the separation between these manifolds in some appropriate way, and showing that they possesses a countable infinities of simple zeroes, independently of the magnitude of the perturbation. For systems with a single degree of freedom, this Melnikov function has a relatively simple form. Let H^0 denote our previous Hamiltonian function H for the unperturbed system, and let H^1 be the perturbation Hamiltonian function. Then the Melnikov function is the line integral of the symplectic Poisson bracket of H^0 and H^1 along an unperturbed homoclinic or heteroclinic orbit and, for our system, is

$$M(\tau_0) = \int_R \{H^0, H^1\}\,[\omega(\tau+\tau_0), \alpha(\tau+\tau_0)]\,d\tau\ , \tag{5.1}$$

where ω is defined as in (3.10) and is a more convenient variable to use than ψ. The horseshoe chaoticity is relatively simple to vizualise on the plane. Typically, consider a homoclinic loop connected to a hyperbolic fixed point on the phase plane (see Figure 5).

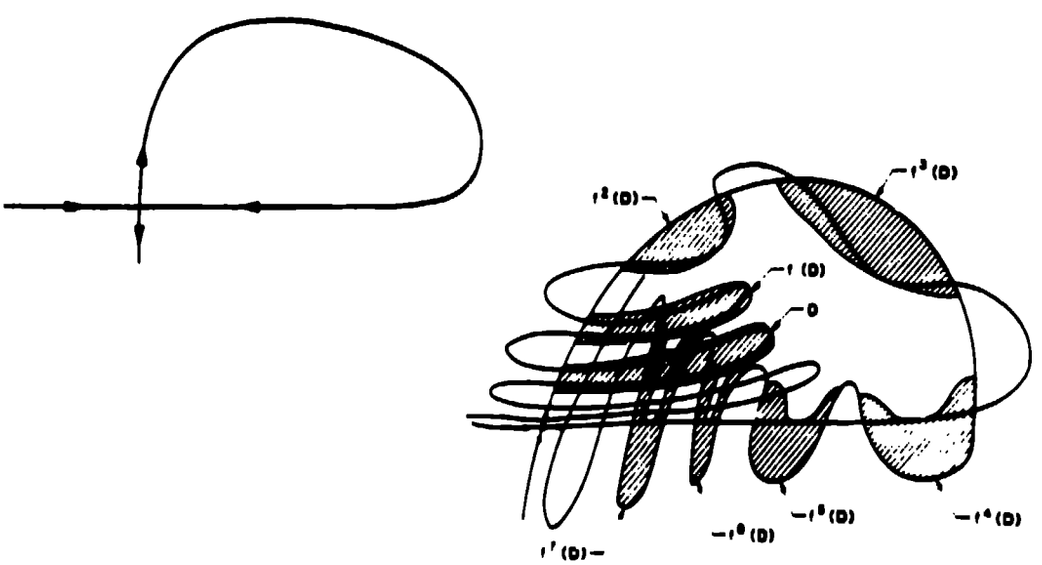

Figure 5. Unperturbed (left) and perturbed (right) dynamics nearby a hyperbolic saddle point.

We consider a perturbation that will preserve the fixed point p, up to a slight displacement. The loop is actually both the stable manifold $W^s(p)$ and the unstable manifold

$W^u(p)$ of p. Generically, under a perturbation, the homoclinic loop will break up so that $W^s(p)$ can no longer be identified with $W^u(p)$, thus giving rise to regions of stochasticity. Two fates are then possible. A first possibility is that these manifolds will miss each other; this does not generate any chaos. The second possibility is that they will intersect transversely (tangential intersection is an intermediate situation). Horseshoe chaos is the consequence of the intersection of these manifolds. In particular, transversal intersection in the Poincaré map induces stretching and folding, as a rectangular region of the phase space is mapped away from and then back into the vicinity of the hyperbolic fixed point. These effects are sufficient to cause horseshoe tangles (see Figure 5 and Wiggins [1988]). A second type of chaotic behaviour is characteristic of dynamics ocuring in higher dimensions and is called Arnold diffusion (see Holmes and Marsden [1982b]). It is characterized by the fact that the phase space is less likely to be partitioned into disconnected regions of stochasticity; indeed this necessitates invariant subspaces of co–dimensions separating the regions. If this condition is not met, then solutions do diffuse from region to region.

The application of the Melnikov technique actually consists in calculating the Melnikov integral and to ascertain whether it has simple zeroes. The existence of chaos generating structure is then a consequence of theorems by Melnikov and Poincaré–Birkhoff–Smale. For systems whose dynamics take place in more than two dimensions, the Melnikov function is no longer given by (5.1). Our perturbations are such that the perturbed systems we are considering here fall within certain classes which are investigated in great detail in Wiggins [1988] and we will present the form of the Melnikov intergal as we go along.

We will now proceed to illustrate the method for three types of perturbations corresponding to the following deformations of the matrix **W**:

$$\mathbf{W} = \mathrm{Diag}\{\lambda_1, \lambda_2 + \epsilon\cos[\nu(\tau - \tau_0)], \lambda_1\}, \tag{5.2a}$$

$$\mathbf{W} = \mathrm{Diag}\{\lambda_1 + \epsilon, \lambda_2, \lambda_1\}, \tag{5.2b}$$

$$\mathbf{W} = \mathrm{Diag}\{\lambda_1 + \epsilon\cos[\nu(\tau - \tau_0)], \lambda_2, \lambda_1\}, \tag{5.2c}$$

where ϵ is small. We will examine the consequence of these perturbations in the neighbourhood of the heteroclinic lines connecting the poles depicted in Figure 2.

Perturbations of type (5.2a) preserve S^2 as the reduced phase space and for this case,

the Melnikov integral is given by (5.1). For the particular case where $\overline{\kappa} = -\kappa$, we find

$$M(\tau_0) = \frac{3r\nu^2\pi}{8\lambda_1^2 \sin^2\alpha_0} \operatorname{csch}\left(\frac{\nu\pi}{4\lambda_1 r \sin\alpha_0}\right) \sin(\nu\tau_0), \tag{5.3}$$

where $\cos\alpha_0 = -(1+L)/2$. Clearly, this expression has simple zeroes located at $\tau_0 = n\pi/\nu$, $n \in Z$. This implies the existence of a Smale horseshoe structure in the Poincaré map, obtained as a recursive folding and stretching of regions nearby the poles. The physical effect implied by the Horseshoe structure is that of an intermittent switching dynamics between two states of circular polarization.

Perturbations of the type (5.2b) break the symmetry that alllowed the second reduction step and thus lift the phase space back to $S^2 \times S^2$. This yields a perturbed system falling within Category III of Wiggins [1988], and for which the Melnikov function is

$$M(\beta_0) = \int_R \frac{\partial H^1}{\partial \beta}(\omega, \alpha, \sigma, \beta + \beta_0)\, d\tau \tag{5.4}$$

Again choosing $\overline{\kappa} = -\kappa$, we find

$$M(\beta_0) = \frac{-r^2(2 - \cos\alpha_0)\sin\beta_0}{\lambda_1 \sin\alpha_0}. \tag{5.5}$$

As in the previous case, this function obviously has simple zeroes and, once again, horseshoe chaos is implied; the difference is that, here, the stable and unstable manifolds are toroidal objects embedded in the space $S^2 \times S^2$. For both of the above types of perturbations, the phase space is partitioned into stochastic dynamical layers separated by invariant tori that form inpenetrable barriers for the polarization.

Finally, perturbations of the type (5.2c) also break symmetries. In contrast with the first two types, it yields Arnold diffusion; the phase space is the five–dimensional manifold $S^2 \times S^2 \times R$ and it can no longer be partitioned in disconnected chaotic regions. Here again, we obtain a system belonging to Category III; however, the Melnikov function is now a vector whose two components are given by

$$\begin{aligned} M_1(\tau_0, \beta_0) &= \int_R \left(\frac{\partial H^0}{\partial \omega}\frac{\partial H^1}{\partial \alpha} - \frac{\partial H^0}{\partial \alpha}\frac{\partial H^1}{\partial \omega} - \frac{\partial H^0}{\partial \sigma}\frac{\partial H^1}{\partial \beta}\right) d\tau + \frac{\partial H^0}{\partial \sigma}\int_R \frac{\partial H^1}{\partial \beta} d\tau, \\ M_2(\tau_0, \beta_0) &= -\int_R \frac{\partial H^1}{\partial \beta} d\tau. \end{aligned} \tag{5.6}$$

Again, choosing $\overline{\kappa} = -\kappa$, we obtain

$$M_1(\tau_0, \beta_0) = \frac{3\nu^2 r\pi(L - \cos\alpha_0 \cos\beta_0)}{16\lambda_1^2 \sin^2\alpha_0} \operatorname{csch}\left(\frac{\nu\pi}{4\lambda_1 r \sin\alpha_0}\right) \sin(\nu\tau_0),$$
$$M_2(\tau_0, \beta_0) = \frac{-\nu\pi(1 - \frac{1}{2}\cos\alpha_0)\sin\beta_0}{4\lambda_1^2 \sin^2\alpha_0} \operatorname{csch}\left(\frac{\nu\pi}{4\lambda_1 r \sin\alpha_0}\right) \cos(\nu\tau_0). \tag{5.7}$$

Here, this pair of functions possesses two distinct sets of zeroes and this is sufficient to ensure the formation of transition chains giving rise to the phenomenon of Arnold diffusion. Physically, this diffusion expresses itself through a back and forth transfer of the polarization among the nonlinear modes of the system in a slow and erratic manner.

6. Conclusions. We presented an investigation of the dynamics of a pair of laser pulses counterpropagating as travelling waves through a nonlinear polarizable medium. We have seen that the geometry of this system is remarkable and that it reduces, for isotropic media, to motion on the sphere, due to continuous Hamiltonian symmetries of the system. We have discovered a set of degenerate bifurcations that can take place in the phase portrait on the reduced space S^2 as material parameters are varied, as shown in Figures 2 and 4. Chaotic behavior under certain classes of spatially periodic perturbations of the optical medium has also been demonstrated by using the Melnikov method. The instance of horseshoe chaos which we examined corresponds to sensitive dynamics on the Poincaré sphere in the form of an intermittent switching from one circular polarization state to the other. We also have shown that Arnold diffusion is another possible chaoticity behaviour under some perturbations that are sufficiently symmetry-breaking.

Outlooks for the work presented here include the addition of dissipative and dispersive effects. In this case, the system must be examined as a set of partial differential equations, thus an infinite-dimensional dynamical system, for which the search for homoclinic structures and mechanisms for the onset of chaotic, or complex, dynamics remains to be done.

References.

V.I. Arnold [1964], Instability of dynamical systems with several degrees of freedom, Sov. Math. Dokl. **156**, 9-12.

M. Crampin and F.A.E. Pirani [1987], *Applicable Differential Geometry*, London Mathematical Society Lecture Notes Series **59**, Cambridge University Press, Cambridge (U.K.).

D. David [1989], Horseshoe chaotic dynamics in a polarized optical beam subject to periodic and dissipative perturbations, Preprint, Los Alamos National Laboratory.

D. David, D.D. Holm, and M.V. Tratnik [1988a], Integrable and chaotic polarization dynamics in nonlinear optical beams, Phys. Lett. **137A**, 355–364.

D. David, D.D. Holm, and M.V. Tratnik [1988b], Horseshoe chaos in a periodically perturbed polarized optical beam, Phys. Lett. **138A**, 29–36.

D. David, D.D. Holm, and M.V. Tratnik [1990], Hamiltonian chaos in nonlinear optical polarization dynamics, Physics Reports (in press).

A.L. Gaeta, R.W. Boyd, J.R. Ackerhalt, and P.W. Milonni [1987], Instabilities and chaos in the polarizations of counterpropagating light fields, Phys. Rev. Lett. **58**, 2432–2435; Instabilities in the propagation of arbitrarily polarized counterpropagating waves in a nonlinear Kerr medium, in *Optical Bistability III*, H.M. Gibbs, P. Mandell, N. Peyghambarian, S.D. Smith (eds.), Springer–Verlag, Berlin.

J. Guckenheimer and P.J. Holmes [1983], *Nonlinear Oscillations, Dynamical Systems, and Bifurcations of Vector Fields*, Applied Mathematical Sciences, Vol. **42**, Springer–Verlag, New–York.

P.J. Holmes and J.E. Marsden [1982a], Horseshoes in perturbations of Hamiltonian systems with two degrees of freedom, Comm. Math. Phys. **82**, 523–544.

P.J. Holmes and J.E. Marsden [1982b], Melnikov's method and Arnold diffusion for perturbations of integrable Hamiltonian systems, J. Math. Phys. **23**, 669–675.

A.E. Kaplan [1983], Light-induced nonreprocity, field invariants, and nonlinear eigenpolarizations, Opt. Lett. **8**, 560–562.

R. Lytel [1984], Optical multistability in collinear degenerate four-wave mixing, J. Opt. Soc. Am. **B1**, 91–94.

P.D. Maker, R.W. Terhune, and C.M. Savage [1964], Intensity-dependent changes in the refractive index of liquids, Phys. Rev. Lett. **12**, 507–509.

V.K. Melnikov [1963], On the stability of the center for time periodic perturbations, Trans. Moscow Math. Soc. **12**, 1–57.

P J. Olver [1986], *Applications of Lie Groups to Differential Equations*, Graduate Texts in Mathematics **107**, Springer–Verlag, New York.

K. Otsuka, J. Yumoto, and J.J. Song [1985], Optical bistability based on self–induced polarization–state change in anisotropic Kerr–like media, Opt. Lett. **10**, 508–510.

M.V. Tratnik and J.E. Sipe [1987], Nonlinear polarization dynamics. I. The single–pulse equations, Phys. Rev. **A35**, 2965–2975; II. Counterpropagating beam equations: new simple solutions and the possiblity for chaos, Phys. Rev. **A35**, 2976–2988; III. Spatial polarization chaos in counterpropagating beams, Phys. Rev. **A36**, 4817–4822.

S. Trillo, S. Wabnitz, and R.H. Stolen [1986], Experimental observation of polarization instability in a birefringent optical fiber, Appl. Phys. Lett. **49**, 1224–1226.

S. Wiggins [1988], *Global Bifurcations and Chaos - Analytical Methods*, Applied Mathematical Sciences **73**, Springer–Verlag, New York.